Mie Scattering Contributions to the Optical Density and Circular Dichroism of T2 Bacteriophage†

G. Holzwarth,* David G. Gordon, James E. McGinness,‡ Burton P. Dorman,§ and Marcos F. Maestre

ABSTRACT: The contributions of Mie scattering to the absorption and circular dichroism (CD) spectra of T2 phage are calculated for a spherically symmetric model of the phage. The diameter of the model is 1000 Å. DNA occupies a central core of diameter 850 Å; this is covered by a protein coat of thickness 75 Å. The optical properties of the protein and DNA are taken from experimental absorption, CD, and optical rotatory dispersion (ORD) curves for disrupted phage, isolated DNA, and isolated protein ghosts. The absorption, scattering, total CD, and scattering contributions to the CD of the model particle are calculated. The calculation yields three conclusions: (1) Mie scattering is the predominant source for the turbidity of suspensions of intact T2 phage; (2) the signs and the shape of the Mie scattering contribution to the CD resemble those observed experimentally, but the observed amplitude of the 280-nm peak is much larger than that calculated and the observed long-wave tail is not found in the calculated curve; (3) the calculated CD curve of the model phage does not accurately yield the observed spectrum of the intact particle. This suggests that a DNA conformational change or long-range asymmetric packing of the DNA, rather than Mie scattering, are the dominant factors generating the observed differences between the CD spectra of intact and disrupted T2 phage.

The secondary structure and packing of DNA in bacteriophage T2 could be elucidated by optical spectroscopy if one understood the observed differences in both the circular dichroism (CD) and in the optical rotatory dispersion (ORD) of intact and disrupted bacteriophage T2 (Maestre and Tinoco, 1967; Maestre *et al.*, 1971). These differences have at least three possible sources: (1) Mie (isotropic particle) scattering due to the particulate nature of the phage suspension; (2) alteration of the optical activity of individual molecules through a change in secondary structure; (3) scattering contributions due to long-range chiral anisotropic packing of the DNA molecules in the phage head. How important is each of these mechanisms? The question can be approached experimentally, as by measurements made with and without the collection of scattered light (Dorman and Maestre, 1973), or by calculation. Our approach here is to estimate by calculation the magnitude of Mie scattering by the phage (first source listed above).

Mie scattering is a direct consequence of the dense packing of DNA in the phage head. The compact structure of the phage causes the refractive index inside the phage to be much greater than in the solvent. This generates large variations in refractive index at various points in the suspension; the refractive index variations lead, in turn, to light scattering effects on absorption and CD spectra. For the sake of the Mie calculation, the phage is modeled by a spherically symmetric particle having an isotropic DNA core and isotropic protein coat of dimensions comparable to those observed. Since Mie theory assumes spherical symmetry, the tail of the phage is deliberately ignored. However, the total mass of protein assumed for the coat includes the mass of the tail. The absorbance, turbidity, circular dichroism, and optical rotation of this model are calculated exactly by a method which has successfully explained particulate effects in the CD of red blood cell ghosts (Gordon and Holzwarth, 1971b) and aggregates of poly(L-glutamic acid) (Gordon, 1972). This method is based on Aden and Kerker's (1951) extension to spherical shells of Mie's (1908) method for evaluating scattering by simple spheres. Maxwell's equations are solved exactly, and no assumptions are made concerning the relative size of particle and wavelength. This is essential, since for ultraviolet (uv) spectroscopy of T2 the particle diameter and light wavelength are of comparable magnitude. Schneider (1971, 1973) has presented a similar method for evaluation of the optical properties of large particles. The calculated spectra are compared to spectra obtained for intact and disrupted phage, measured by a novel technique which allows essentially all of the scattered light to be collected (Dorman and Maestre, 1973; Dorman *et al.*, 1973).

Experimental Section

T2 bacteriophage was chromatographed on a hydroxylapatite column and then dialyzed against a solution containing 0.5 M NaCl, 1 mM $MgSO_4$, and 1 mM Tris-HCl at pH 6.8, as previously described (Maestre *et al.*, 1971; Dorman and Maestre, 1973). Phages were disrupted by freeze–thawing. This procedure leads to release of DNA into the dialysis buffer. The protein coat and tail remain intact as a "ghost." Viral DNA was extracted with phenol followed by dialysis against 0.1 M NaCl in 10 mM sodium–phosphate buffer at pH 7.2.

† Contribution from the Department of Biophysics (G. H.) and the Department of Chemistry (D. J. G. and J. E. M.), University of Chicago, Chicago, Illinois 60637, and from the Department of Chemistry (B. P. D.), and the Space Sciences Laboratory (M. F. M.), University of California, Berkeley, California 94720. *Received September 10, 1973.* The research at the University of Chicago has been supported by the National Institutes of Neurological Diseases and Stroke through Grant NS-07286. The work at the University of California was supported by NASA Grant 05-003-020 and by National Institutes of Health Grants AI-08427-04 and GM-11180. G. H. is grateful for the support of Research Career Development Award GM-15050 from the National Institutes of Health. D. J. G. is pleased to acknowledge support by U. S. Public Health Service Training Grant No. HD-00001 from the National Institute of Child Health and Human Development.

‡ Present address: Department of Chemistry, University of California, La Jolla, Calif. 92037.

§ Present address: Department of Biology, Yale University, New Haven, Conn. 06520.

Optical density curves were measured in a standard cuvet by a normal Cary 14 spectrophotometer. Although this instrument undoubtedly collects part of the scattered light, we assume that the fraction of scattered light collected is small, and we designate spectra thus obtained as A_T, representing total (absorptive and scattering) optical density. To obtain true absorption spectra free of the effects of light scattering, the sample was placed in a special fluorscat optical cell (Dorman *et al.*, 1973) in Cary 1462 scattered transmission accessory. Absorbance curves thus obtained are labeled A_A. The contribution of scattering to the measured optical density is labeled A_S and is equal to $A_T - A_A$.

Circular dichroism curves with and without collection of scattered light were similarly obtained. The circular dichroism measured in the usual way with a standard cuvet, in a Cary 6001 or 6003 CD instrument, is designated θ_T on the assumption that no scattered light is accepted by the detector. CD measurements in which scattered light and transmitted light were collected, yielding θ_A, the absorptive part of the circular dichroism, were obtained using a fluorscat cell in a Cary 6001 instrument. The scattering contribution to circular dichroism, θ_S, is given by $\theta_T - \theta_A$. Occasionally, measurements of θ_T were obtained by placing a large-area photomultiplier tube directly adjacent to the sample cuvet. Data similar to those of the fluorscat technique were obtained.

Optical rotation data, Φ, measured with a standard cuvet in a Cary 60 spectropolarimeter, were taken from previously published work (Maestre and Tinoco, 1967); no correction was made for scattering.

Calculations

The calculations are performed for a spherically symmetric model of the virus, as shown in Figure 1. The total radius of the particle, R, is taken as 500 Å, in accord with the average radius of the phage head (Brenner *et al.*, 1959; Cummings and Kozloff, 1962). (A recent review by Cummings *et al.* (1970) suggests that 400 Å would be a better average radius; this radius yields results differing only slightly from those for the 500-Å radius, as discussed later.) The particle is composed of a protein coat of thickness Δ and a DNA core of radius $R - \Delta$. The value of Δ was chosen as 75 Å; electron microscopic evidence suggests that the protein layer is 60–80 Å thick (Kellenberger *et al.*, 1968). There are thus three regions of space for the calculation: 1 = DNA core, 2 = protein coat, and 3 = external solvent. For each region of space we need to know the complex refractive index for left and right circularly polarized light; these are designated m_{1L}, m_{1R}, m_{2L}, m_{2R}, etc. After the refractive indices are specified, one can obtain, by a rigorous, straightforward calculation, the total optical density A_T, the scattering A_S, and the absorbance A_A, for a suspension of particles. The total optical density A_T is calculated by considering the detector to accept only transmitted light and light which is scattered at zero angle. The scattering contribution to the optical density, labeled A_S, is obtained by integrating the scattered radiation for all scattering angles. Finally, the absorptive contribution A_A is evaluated simply as $A_T - A_S$. The quantity A_A corresponds to a measurement of absorbance in an instrument which collects the transmitted light and all scattered light (4π sr).

In a similar fashion, the Mie calculation yields the total, scattering, and absorptive circular dichroism θ_T, θ_S, and $\theta_A = \theta_T - \theta_S$. The quantity θ_T corresponds to a CD measurement by an instrument whose detector collects only transmitted light and light scattered directly forward; θ_A corresponds to a CD measurement in which transmitted light and all scattered light reach the detector.

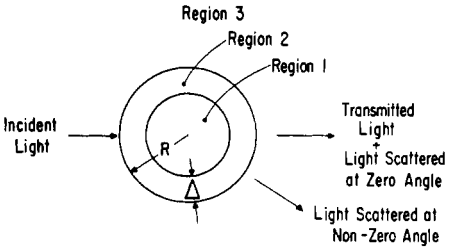

FIGURE 1: The spherically symmetric structure used in the calculations to model T2 phage. The outer particle radius R is 500 Å. Region 1, the core, of radius $R - \Delta$, is occupied by DNA and water; region 2, of thickness $\Delta = 75$ Å, is occupied by protein and water. Region 3 is occupied by water alone. For light incident from the left, a detector placed an infinite distance away toward the right would see only transmitted light and light scattered at zero angle. By contrast, light scattered at nonzero angles will also be accepted if a large area detector is placed close behind the scatterer or if the scatterer is placed in a fluorscat cell.

The method used to evaluate the complex refractive indices at a given wavelength λ is as follows. For region 1, the DNA core, we use a mean dielectric constant containing contributions from both water and DNA. The contribution of DNA is estimated by evaluating the Kronig–Kramers transform K of the absorption spectrum of isolated, B-form T2 DNA. We use the measured absorption spectrum between 190 and 350 nm and extrapolate the data to zero at 140 nm. To the term K we add the Kronig–Kramers transform of a lumped absorption band at 120 nm, giving a term $Q\lambda^2/(\lambda^2 - \lambda_0^2)$. The size Q of the second band is adjusted to yield dn/dc equal to 0.188 ml/g at 435.8 nm, as observed (Reichmann *et al.*, 1954). For any desired DNA concentration c in grams per milliliter one has

$$\epsilon_1(c) = 1 + (\epsilon_{H_2O} - 1)(1 - c\bar{v}) + c\bar{v}(K + Q\lambda^2/[\lambda^2 - \lambda_0^2]) \quad (1)$$

Here $\bar{v}$ is the partial specific volume of DNA, taken as 0.55 cm^3/g (Hearst, 1962). The value of c is fixed by the core size and the known molecular weight of the T2 DNA, 1.2×10^8 daltons (Stent, 1963). The mean real refractive index of region 1, n_1, is just $\epsilon_1^{1/2}$.

The complex refractive indices for left and right circularly polarized light are then evaluated, in the manner previously described (Gordon and Holzwarth, 1971b; Gordon, 1972), as follows

$$m_{1L} = \tilde{n}_1 - i\lambda 2.303A_1/4\pi NV_1 + \lambda(\Phi_1 - i\theta_1)/360NV_1 \quad (2)$$

$$m_{1R} = \tilde{n}_1 - i\lambda 2.303A_1/4\pi NV_1 - \lambda(\Phi_1 - i\theta_1)/360NV_1 \quad (3)$$

Here V_1 is the volume of the core. A_1, Φ_1, and θ_1 are the absorbance (base 10), ORD (degrees), and CD (degrees) of a T2 DNA solution for a 1-cm path and a standard concentration, which we took as 10^{-4} M in nucleotide (or $N = 1.9 \times 10^{11}$ phage/cm^3). The absorbance, ORD, and CD data were all measured by normal methods in standard cuvets, since these solutions do not scatter light significantly.

The refractive indices for region 2 are calculated similarly. The mean dielectric constant of pure protein is approximated by the Kronig–Kramers transform of a Gaussian absorption band at 190 nm (maximum molar absorptivity 10^4 M^{-1} cm^{-1};

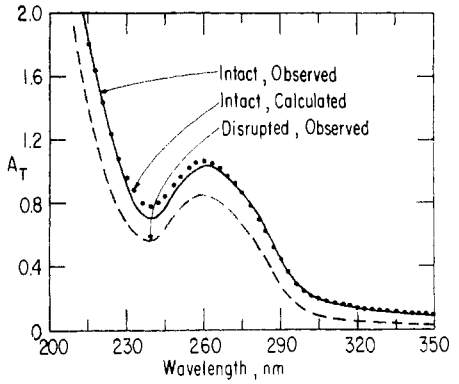

FIGURE 2: The observed optical density spectrum A_T of intact (—) and disrupted (- - -) T2 phage, and the corresponding spectrum A_T calculated for intact phage (· · ·). The data include the effects of light lost by scattering and by absorption. Phage concentration: 10^{-4} M in nucleotides (1.87×10^{11} phages/ml). Observed data were measured with Cary 14 in a standard 1-cm cuvet.

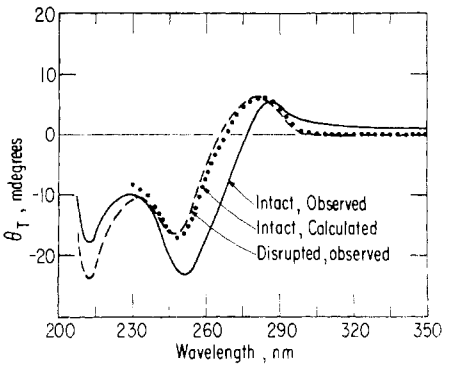

FIGURE 4: Circular dichroism of intact and disrupted T2 phage as measured by normal methods: (—) CD (θ_T) for intact phage as measured with a Cary 6003 using standard cuvet; (· · ·) θ_T calculated for our model of the intact phage; (- - -) CD measured for disrupted phage using a standard cuvet in a Cary 6001 instrument: path length, 1 cm; concentration, 10^{-4} M in nucleotides. The CD is given in millidegrees of ellipticity.

bandwidth 12 nm) and an additional band at 120 nm with intensity Q'. The value of Q' is adjusted to yield dn/dc = 0.194 ml/g at 435.8 nm; this value of dn/dc is an average of published values for a variety of proteins (Doty and Edsall, 1959). The dielectric constant for a given shell geometry, assuming a protein mass of 9×10^7 daltons (Stent, 1963), is evaluated by the analog of eq 1. The partial specific volume of protein was taken as 0.72 cm^3/g (Tanford, 1961).

The complex refractive indices for left and right circularly polarized light are then evaluated by eq 2 and 3, but with A_1 replaced by A_2 (the absorbance of T2 ghosts), Φ_1 replaced by Φ_2 (T2 ghost rotation), and θ_1 replaced by θ_2, the ghost CD. The ghost CD was obtained by subtracting the CD of DNA from the CD of disrupted phage as measured with fluorscat optics. Both A_2 and θ_2 are measured by methods which eliminate the effects of scattering; Φ_2 is not so corrected, but the error introduced should be small in the spectral region of interest. The refractive index m_3 is that of the solvent, water, so $m_{3R} = m_{3L}$. The values of m_3 are interpolated from data in the International Critical Tables.

The real mean refractive indices at several wavelengths of the DNA core, protein coat, and water, in that order, are as follows: λ 350, $\bar{n}_1 = 1.473$, $\bar{n}_2 = 1.496$, $\bar{n}_3 = 1.349$; λ 300, 1.504, 1.516, 1.359; λ 250, 1.509, 1.555, 1.377; λ 220, 1.569, 1.609, 1.398. These refractive indices correspond to a DNA concentration of 0.623 g/ml and a protein concentration of 0.736 g/ml as dictated by the particle geometry.

With the above specifications for R, Δ, m_{1L}, m_{1R}, m_{2L}, m_{2R}, and m_3, the optical spectra A_T, A_S, A_A, θ_T, θ_S, θ_A, and Φ of the model T2 phage suspension are readily calculated by Mie theory (Gordon, 1972; eq 5, 10, and 13–21). These results may then be compared to the respective observed spectra of T2 phage.

Results

The experimental data to be explained, and the results of the Mie calculations, are presented in Figures 2–5. Figure 2 shows the experimental total optical density (absorbance plus scattering), A_T, for intact phage and for disrupted phage. There is substantially greater optical density observable in

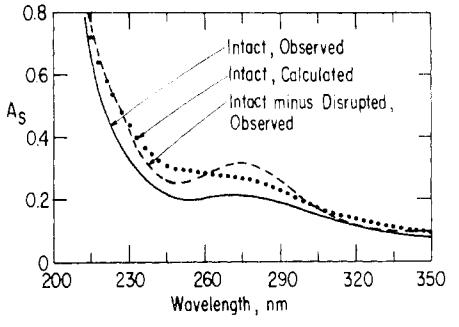

FIGURE 3: The contribution of scattering to the optical density of T2 phage: (—) intact phage, optical density measured with Cary 14 in standard cuvet, *minus* optical density measured in fluorscat cell with Cary 1462 scattered light collection accessory; (· · ·) scattering contribution A_S calculated for intact phage; (- - -) optical density of intact phage measured with standard cuvet in Cary 14, minus absorption of disrupted phage measured with fluorscat cell in a Cary 1462. The dashed curve may reflect several other factors in addition to scattering. Path length, 1 cm; concentration, 10^{-4} M in nucleotides.

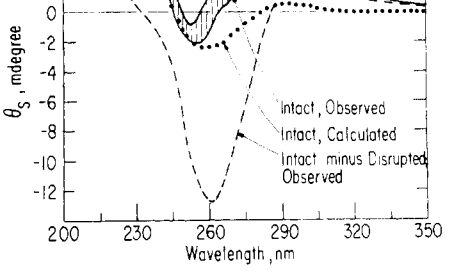

FIGURE 5: Scattering contributions to the circular dichroism of T2 phage. The two solid lines are two separate experiments evaluating θ_S for intact phage. Each shows the difference between CD measured for intact phage with standard cuvet *minus* the CD measured for intact phage with Cary 6001 using fluorscat optical cell. Dots show the calculated scattering contribution θ_S to the CD of our model of the intact phage. The dashed curve gives the difference between CD measured for intact phage in a standard cuvet with Cary 6003 minus the CD measured for disrupted phage in a Cary 6001 using a standard cuvet and a close detector. The disrupted phage CD spectrum has been shown to be independent of the detection geometry (Dorman and Maestre, 1973). Path length, 1 cm; phage concentration 10^{-4} M in nucleotides. The units of θ are millidegrees of ellipticity.

the intact phage than in disrupted phage for all wavelengths shown. The intact phage spectrum shows a pronounced tail for $\lambda > 320$, which arises from scattering.

The calculated values of A_T for our model of the intact phage are also shown in Figure 2. The calculations are seen to fit the observed A_T quite closely; the long-wave tail and the detailed shape of the enhancement in optical density, both of which are due to scattering, are nicely predicted by our model.

The role of scattering in the absorption spectra can also be studied experimentally using the fluorescent scattering technique (Dorman and Maestre, 1973). The value of A_S for intact phage, evaluated by subtracting the measured absorbance of T2 suspension in a fluorscat cell from that for a normal cuvet, is shown in Figure 3. The experimental curve shows a substantial tail for $\lambda > 320$, a level region from 290 to 245 nm, and then rises sharply. The calculated values of A_S are seen to agree closely in magnitude and shape with the observed curve. This result supports the view that for intact T2 phage, the scattering contribution to optical density is largely a consequence of dense packing of DNA inside the phage head. By contrast, the difference between A_T for intact phage and A_A for disrupted phage, also given in Figure 3, shows a small peak at 275 nm and a modest dip at 245 nm. These features, which are not as prominent in the experimental and calculated A_S curves, originate in a 2-nm red-shift of the absorption maximum of the DNA in intact phage compared to that of the disrupted particle. In addition, the enhanced amplitude of the difference between A_T for intact phage and A_A for disrupted phage reflects an 11% absorbance increase (hyperchromic shift) of the DNA in the intact phage relative to the solution spectrum of B-DNA. This hyperchromism is discussed further below.

The corresponding experimental and calculated total CD curves (absorptive plus scattering), θ_T, are shown in Figure 4. Consider first the experimental data for intact phage. These show a pronounced long-wave tail, a modest, positive peak at 288 nm, and a large, negative trough with a minimum at 250 nm. The curve is distinctly nonconservative. By contrast, the disrupted phage, with B-form DNA, shows no scattering tail. The 280-nm peak is larger, while the 248-nm trough is shallower than that for the intact phage, leading to a more conservative CD curve for the 260-nm absorption region. The calculated CD for the intact phage, also shown in Figure 4, closely resembles the CD of the disrupted phage. Neither the long-wave CD tail of the intact phage, nor the nonconservative shape of the CD curve, is reproduced by the calculation. We conclude that the observed difference between θ_T for intact and disrupted phage cannot originate solely from the particulate, dense packing of DNA in the phage head.

In Figure 5 are shown the corresponding experimental and calculated curves of θ_S, the scattering contribution to the circular dichroism. The experimental value of θ_S for intact phage is evaluated by subtracting the absorptive CD, measured by the fluorscat method, from the CD measured with normal optics. There is no change in particle structure between the two measurements. The experimental θ_S curve shows a 4–5-mdeg positive peak near 280 nm, a trough, -1 to -2 mdeg, near 255 nm, and then a positive peak again at wavelengths shorter than 245 nm. The calculated θ_S curve shows a positive peak, $+0.6$ mdeg, at 290 nm, a negative trough, -2.4 mdeg, at 257 nm, and positive CD for $\lambda < 245$ nm. The observed and calculated curves thus have the same basic shape, although the magnitude of the positive scattering peak for $\lambda > 270$ differs in the two cases. This suggests that a substantial part of the experimental θ_S may originate in the same physical properties which give rise to Mie scattering from T2 phage. It is useful to contrast this result with the observed difference between experimental θ_T curves for intact and disrupted phage, also shown in Figure 5. This curve has a small positive peak at 300 nm, a very large negative trough, -13 mdeg, at 260 nm, and positive CD for $\lambda < 230$. This curve is not accounted for by the Mie scattering calculation or by the observed θ_S.

How sensitive are the calculated curves to the particular parameters chosen to represent the phage? We have performed similar calculations with the refractive index of protein and/or DNA incremented by 0.1. The calculated values of A_T and A_S obtained systematically exceed the observed by a substantial amount, so we believe our original refractive indices to be accurate. The amplitude of the θ_S curve is increased by larger n, but the θ_T and θ_S curves are not qualitatively altered and our conclusions on the fit between theory and experiment would remain unchanged.

We have also varied the particle radius to 400 and 600 Å, and the protein coat thickness to 50 and 100 Å. The qualitative results obtained are consistent with the increased or decreased refractive indices which automatically follow from eq 1 when a fixed amount of DNA or protein is confined to a larger or smaller compartment volume. Again no significant improvement in the fit of calculated CD curves to the observed could be achieved without the calculated A_S grossly exceeding that observed.

We note that all of our Mie calculations have been performed using complex refractive indices derived from disrupted phage, for which the DNA is in the B conformation. It would be desirable to use molecular properties appropriate to the conformation of the DNA in the phage. Indeed, data for the CD and absorption curves of the DNA and protein of intact phage, free from the effects of scattering, packing, and absorption flattening, are a goal of the present study. However, we elected not to use as input data for eq 2 and 3 CD and absorption curves measured on intact phage with fluorscat optics because we do not have available as input for the Mie calculations corresponding experimental ORD curves for intact phage which are free of scattering effects. Since the calculated scattering contribution θ_S is of the same shape as the input ORD curve for the DNA, an undistorted input ORD is essential to the calculation of θ_S. However, the resemblance of θ_S to the input ORD (Gordon, 1972) allows the reader to readily gauge the shape of the calculated θ_S curve which would result from assuming different DNA conformation. In particular, if C-form data were used as input to the Mie calculation, the positive peak in the calculated θ_S near 290 nm would largely disappear, giving, for $\lambda > 280$ nm, a poorer fit between the experimental and the calculated θ_S curves.

Discussion

Mie Scattering. We are now in a position to answer several questions about the absorption and CD spectra of T2 and about the structural interpretation of these spectra. First, we assert that the scattering contribution to optical density, A_S, can be fully accounted for by the dense particulate nature of T2 phage. It is not necessary to invoke internal structure (anisotropy) of the DNA in the phage; such structure might be expected to yield enhanced scattering (Tinker, 1972). However, we cannot with confidence turn the argument around to assert that our results support a nonstructured packing of DNA in the phage, since the scattering from

spinach chloroplasts, which are known to be highly structured, can be largely explained by Mie calculations for an isotropic model (Bryant *et al.*, 1969). The difference in optical density A_T for intact and disrupted phage (the dashed curve in Figure 3) appears to originate largely in Mie-type isotropic particle scattering, but additional factors, which are discussed below, must also be involved.

Turning next to circular dichroism, we note in Figure 4 that the calculated CD curve does not fit the CD of intact phage. Instead, it resembles the CD of disrupted phage, *i.e.* it resembles closely the data used as input to the calculation. Thus Mie scattering, which was invoked in the introductory statement as one of three possible sources to explain the difference between the CD of intact and disrupted phage, cannot explain the effects entirely, although its contribution is nonnegligible.

Is it possible that our neglect of the phage tail has led to a gross underestimate of the CD contributions arising from the dense, particulate nature of the phage? Experiments show that the phage ghost, which retains the tail, exhibits negligible CD between 245 and 350 nm (B. P. Dorman and M. F. Maestre, manuscript in preparation). The tail thus cannot play a major role in the CD of the intact phage.

Secondary Structure vs. Anisotropic Packing. Let us turn from the primary subject of this manuscript, Mie scattering, to consider the other factors which could play a significant role in the CD of intact phage. In so doing, we enter an area of suggestive rather than definitive experimental data; reasonable and prudent persons, not excluding the authors, may differ in their conclusions. The recently reported crystallization of T4 phage (Speyer and Khairallah, 1973) suggests that X-ray diffraction analysis may soon provide information which will dispel our present uncertainty about the secondary conformation of DNA inside the phage.

We consider first three experimental observations supporting the viewpoint, first adopted by Maestre and Tinoco (1967), that secondary structural changes play a major role in the CD changes accompanying phage disruption.

(A) Similarities between the CD spectra of C-form films (Tunis-Schneider and Maestre, 1970) and the fluorscat CD spectra of intact phage suggest that DNA in the phage is in C conformation (Dorman and Maestre, 1973). Both spectra show very little CD for $\lambda > 280$ nm, in contrast to B-form DNA, which shows a large positive band in this spectral region. Moreover, the intrinsic CD of B- and C-form DNA have been shown to originate in large terms of opposite sign which nearly cancel (Johnson and Tinoco, 1969). Thus it can be argued that small changes in helix geometry, such as an alteration of the base–tilt angle, could lead to large changes in the CD. The persuasiveness of the C-DNA assignment is moderated by the observation that the major 250-nm trough, -7 mdeg deep in the CD of intact T2 phage, is not quite so prominent (-3.5 mdeg) in the C-form spectra of calf thymus DNA films (Dorman and Maestre, 1973; Tunis-Schneider and Maestre, 1970). However, this difference quite probably is due to the extensive (70%) glucosylation of T2 DNA, which has been shown to be the dominant cause of enhancement of the DNA CD troughs at 210 and 245 nm (Usatyi and Shlyakhtenko, 1973).

(B) Spectrophotometric data demonstrate that DNA inside T2 and T6 phage possesses an OD_{260} 33% greater than the same DNA in the B-form conformation (Rubenstein *et al.*, 1961; Bonhoeffer and Schachman, 1960). In more recent work, Tikchonenko *et al.* (1966) have shown spectrophotometrically that this change originates not only in changes in scattering, but also in 11% hypochromicity upon release of the phage DNA. These results are corroborated by our own work with the fluorscat technique, which yields a total optical density loss of 32±% upon T2 disruption and an 11% drop between the fluorscat spectra of intact and disrupted T2 (B. P. Dorman and M. F. Maestre, manuscript in preparation). We interpret these absorption data as evidence for a DNA conformational change.

(C) The magnetic CD spectrum of intact T2 phage exhibits no sign of a long-wavelength tail but does show spectral properties which can in some respects be mimicked by the hyperchromic DNA conformation produced through partial heat denaturation *in vitro* (Maestre *et al.*, 1971). This is evidence that conformational change occurs upon phage disruption.

The evidence favoring CD contributions from anisotropic packing of DNA in the intact phage is as follows. As we have noted above, the calculated Mie scattering contribution to the CD of intact phage, Figure 5, fails to explain the large, positive, long-wave tail in the observed θ_S and θ_T curves. This discrepancy probably does not originate in the assumption of sphericity, since the absorption curve is nicely fitted. Conformational change cannot explain the discrepancy for nonabsorptive regions ($\lambda > 320$). Moreover, conformational change is an unlikely source of the discrepancy for $270 < \lambda < 320$, since this would require that the DNA inside the phage has ORD more positive than B-form DNA for $\lambda > 280$ nm. The available data, admittedly not corrected for scattering, suggest instead that the DNA in the phage has negative ORD in this region (Maestre and Tinoco, 1967). Correction of these data for Mie scattering can be estimated from our calculations; the net ORD would probably remain negative for $\lambda > 280$, unlike the ORD data for the B form.

It is interesting to note parenthetically that, in contrast to the present case, anisotropic structure need not always be invoked to explain the CD of light scattering specimens. For example, the spectral differences between CD curves for intact and dispersed red blood cell ghosts *are* explicable by a Mie calculation similar to the one performed here for T2 (Gordon and Holzwarth, 1971b). The red blood cell ghost calculation assumes an isotropic, spherically symmetric model although one knows that the membrane must be optically anisotropic due to lipid and perhaps protein orientation in the plane of the membrane. One may speculate that anisotropy is of little influence on the red cell ghost spectra for two reasons. (1) The large radius of curvature (35,000 Å) and small membrane thickness (70 Å) combine to yield a particle which behaves optically like two independent 70-Å thick sheets. This thickness is much less than the wavelength. (2) The intrinsic CD of the membrane proteins is large compared to their absorbance, whereas the linear dichroism of the membranes is probably small. A calculation of the effects of anisotropy on scattering by 300-Å diameter, hollow phospholipid vesicles (Tinker, 1972) suggests a somewhat contrary view, but the ratio of thickness to diameter is much larger for the vesicles than for the red cell ghost.

What sorts of optical effects can anisotropy generate in CD spectra? It has been shown by several groups (Saeva and Wysocki, 1971; Saeva, 1972; Schrader and Korte, 1972; Sackmann and Voss, 1972; Dudley *et al.*, 1972; Chabay, 1972) that cholesteric liquid crystals exhibit relatively enormous CD and ORD bands centered approximately at the frequency of each of their absorption bands when studied by light propagating parallel to the cholesteric helix axis. (These bands occur in addition to the well-known optically active reflection band

(de Vries, 1951) which appears, generally in nonabsorptive spectral regions, when the light wavelength in the medium equals the helix pitch.) It is found that the CD band shapes generally resemble those of the absorption bands, but with a "hook," often generating CD of opposite sign, at their long- or short-wave edge (Chabay, 1972; Holzwarth *et al.*, 1973). This hook arises from the birefringence dispersion generated by the absorption band itself (Holzwarth and Holzwarth, 1973).

The CD effects of a randomly oriented collection of small liquid crystallites, such as could perhaps occur in T2 suspension, are at present not known; the experiments and theory for the liquid crystal CD in absorptive spectral regions have, so far, been confined to normal incidence on single crystals. However, recent studies of the CD of randomly oriented spinach chloroplasts and of polylysine–DNA complexes show instructive similarities to the CD of simple liquid crystals, as follows. Philipson and Sauer (1973) have shown experimentally that spinach chloroplasts exhibit very large CD effects in the 680-nm region of chlorophyll absorption. The CD bands possess tails extending into nonabsorptive spectral regions. The large CD effects are not eliminated when scattered light is collected in the CD measurement; instead, the bands change sign. However, when the supramolecular order (grana structure) of the chloroplast is broken down by sonication, the CD diminishes in amplitude by a factor of 10. Philipson and Sauer (1973) suggest that the large-amplitude CD of the intact chloroplast originates primarily in the ordered arrangement of chromophores into a grana structure rather than in the optical activity of individual chlorophyll molecules.

Similarly, studies of compact poly-L-lysine–DNA complexes (Cohen and Kidson, 1968; Shapiro *et al.*, 1969; Haynes *et al.*, 1970) show large nonconservative CD bands with maximum amplitude near 260 nm. The shape of the CD bands is strikingly similar to that of intact T2, yet X-ray diffraction studies indicate that the particles, which are comparable in size to T2, contain B-form DNA (Haynes *et al.*, 1970). Felsenfeld and coworkers (Shapiro *et al.*, 1969) and Gratzer and coworkers (Haynes *et al.*, 1970) suggest, as one possible explanation of their CD data, that the DNA in the particles might possess an ordered anisotropic supramolecular, perhaps liquid crystalline, arrangement.

The CD spectra of suspensions of chloroplasts and of polylysine–DNA complexes thus share three features with the CD curves of liquid crystals: (1) CD amplitudes apparently much larger than those intrinsic to their molecular constituents; (2) CD extending to nonabsorptive spectral regions; (3) CD band shapes closely resembling the absorption spectrum but with a hook of opposite sign.

Applicability of the liquid crystal results to T2 bacteriophage is not as convincing, since, for T2, the amplitude of the CD spectrum is only slightly greater in the intact particle than in the disrupted phage (item 1 above). However, strong scattering is observed well into the visible (item 2). This scattering cannot originate in the intrinsic CD of any particular DNA secondary structure or, as we now know, in Mie scattering. Finally, the difference CD spectrum between intact and disrupted phage (Figure 5, dashed line) bears a strong similarity to a DNA absorption curve, but with a hook at longer wavelengths (item 3 above).

Summary

Mie scattering calculations for a model of T2 bacteriophage demonstrate three points. (1) The contributions of scattering to the optical density of T2 phage suspensions are correctly predicted by Mie theory. This suggests that the dense, particulate nature of the phage is the predominant source of scattering contributions to the OD. (2) The contributions of Mie scattering to CD of intact T2 phage are calculated to be +0.6 mdeg at 290 nm and −2.4 mdeg at 257 nm for a 1-cm path through a suspension 10^{-4} M in nucleotides. The corresponding experimental values of the scattering are 2.5–3.5 mdeg at 290 nm and 0 to −2 mdeg at 257 nm. The calculated CD spectral shape resembles the observed scattering curve broadly. However, it fails to explain the experimental scattering amplitude at 280 nm (4–5 mdeg) or the extent of the observed long-wave tail. (3) The calculated CD for intact phage, using as input data the spectra of disrupted phage, does not describe accurately the observed CD spectrum of the intact particle. The difference is believed to arise from a combination of conformational change and from supramolecular ordering. It is noted that the difference CD curve is similar in shape to CD curves observed at the absorption bands of liquid crystals.

Acknowledgments

We are grateful to K. D. Philipson and K. Sauer for a preprint of their provocative work on chloroplast CD.

References

Aden, A. L., and Kerker, M. (1951), *J. Appl. Phys. 22*, 1242.
Bonhoeffer, F., and Schachman, H. K. (1960), *Biochem. Biophys. Res. Commun. 2*, 366.
Brenner, S., Streisinger, G., Horne, R. W., Champe, S. P., Barnett, L., Benzer, S., and Rees, M. W. (1959), *J. Mol. Biol. 1*, 281.
Bryant, F. D., Seiber, B. A., and Latimer, P. (1969), *Arch. Biochem. Biophys. 135*, 97.
Chabay, I. (1972), *Chem. Phys. Lett. 17*, 283.
Cohen, P., and Kidson, C. (1968), *J. Mol. Biol. 35*, 241.
Cummings, D. J., Couse, N. L., and Forrest, G. L. (1970), *Advan. Virus Res. 16*, 1.
Cummings, D. J., and Kozloff, L. M. (1962), *J. Mol. Biol. 5*, 50.
Day, L. A., and Hoppensteadt, F. (1972), *Biopolymers 11*, 2131.
de Vries, H. (1951), *Acta Crystallogr. 4*, 219.
Dorman, B. P., Hearst, J. E., and Maestre, M. F. (1973), *Methods Enzymol. 27D*, 767.
Dorman, B. P., and Maestre, M. F. (1973), *Proc. Nat. Acad. Sci. U. S. 70*, 255.
Doty, P., and Edsall, J. (1959), *Advan. Protein Chem. 6*, 55.
Dudley, R. J., Mason, S. F., and Peacock, R. D. (1972), *J. Chem. Soc., Chem. Commun.*, 1084.
Gordon, D. J. (1972), *Biochemistry 11*, 413.
Gordon, D. J., and Holzwarth, G. (1971b), *Proc. Nat. Acad. Sci. U. S. 68*, 2365.
Haynes, M., Garrett, R. A., and Gratzer, W. B. (1970), *Biochemistry 9*, 4410.
Hearst, J. E. (1962), *J. Mol. Biol. 4*, 415.
Holzwarth, G., Chabay, I., and Holzwarth, N. A. W. (1973), *J. Chem. Phys. 58*, 4816.
Holzwarth, G., and Holzwarth, N. A. W. (1973), *J. Opt. Soc. Amer. 63*, 324.
Johnson, C., and Tinoco, I., Jr. (1969), *Biopolymers 7*, 727.
Kellenberger, E., Eiserling, F. A., and Boy de la Tour, E. (1968), *J. Ultrastruct. Res. 21*, 335.

Maestre, M. F., Gray, D. M., and Cook, R. B. (1971), *Biopolymers 10*, 2537.
Maestre, M. F., and Tinoco, I., Jr. (1967), *J. Mol. Biol. 23*, 323.
Mie, G. (1908), *Ann. Phys. (Leipzig) 25*, 377.
Philipson, K. D., and Sauer, K. (1973), *Biochemistry 12*, 3454.
Reichmann, M. E., Rice, S. A., Thomas, C. A., and Doty, P. (1954), *J. Amer. Chem. Soc. 76*, 3047.
Rubenstein, I., Thomas, C. A., Jr., and Hershey, A. D. (1961), *Proc. Nat. Acad. Sci. U. S. 47*, 1113.
Sackmann, E., and Voss, J. (1972), *Chem. Phys. Lett. 14*, 528.
Saeva, F. D. (1972), *J. Amer. Chem. Soc. 94*, 5135.
Saeva, F. D., and Wysocki, J. J. (1971), *J. Amer. Chem. Soc. 93*, 5928.
Schneider, A. S. (1971), *Chem. Phys. Lett. 8*, 604.
Schneider, A. S. (1973), *Methods Enzymol. 27D*, 751.
Schrader, B., and Korte, E. H. (1972), *Angew. Chem. 84*, 218; *Angew. Chem., Int. Ed. Engl. 11*, 226.
Shapiro, J. T., Leng, M., and Felsenfeld, G. (1969), *Biochemistry 8*, 3219.
Speyer, J. F. and Khairallah, L. H. (1973), *J. Mol. Biol. 76*, 415.
Stent, G. (1963), Molecular Biology of Bacterial Viruses, San Francisco, Calif., W. H. Freeman.
Tanford, C. (1961), The Physical Chemistry of Macromolecules, New York, N. Y., Wiley.
Tikchonenko, T. I., Dobrov, E. N., Velikodvorskaya, G. A., and Kisseleva, N. P. (1966), *J. Mol. Biol. 18*, 58.
Tinker, D. O. (1972), *Chem. Phys. Lipids 8*, 230.
Tunis-Schneider, M. J. B., and Maestre, M. F. (1970), *J. Mol. Biol. 52*, 521.
Usatyi, A. F., and Shlyakhtenko, L. S. (1973), *Biopolymers 12*, 45.

Mechanism of Action of Naturally Occurring Proteinase Inhibitors. Studies with Anhydrotrypsin and Anhydrochymotrypsin Purified by Affinity Chromatography†

Harry Ako,‡ Robert J. Foster, and Clarence A. Ryan*,§

ABSTRACT: Anhydrochymotrypsin and anhydrotrypsin are enzymatically inert derivatives of trypsin and chymotrypsin in which the active-site serine residues have been converted to sterically smaller dehydroalanine residues. The identity of the anhydroenzymes, purified by affinity chromatography, was established by quantitative recovery of pyruvate from acid hydrolysates and by quantitative recovery of [^{3}H]alanine from NaB^{3}H$_4$-treated proteins. Additional evidence of the purity of the anhydroenzymes was obtained by their stoichiometric binding with natural proteinase inhibitors. There was a strong difference maximum near 245 nm when the absorption spectra of denatured anhydrotrypsin and anhydrochymotrypsin were compared with the absorption spectra of the two unmodified, native enzymes. The circular dichroic (CD) spectra of purified anhydrochymotrypsin and native chymotrypsin were nearly identical but differed significantly from the denatured enzymes. The thermodynamics of the protein–protein interactions between the anhydroenzymes and naturally occurring proteinase inhibitors were investigated using an equilibrium, competitive binding technique. The binding of virgin soybean trypsin inhibitor, modified soybean trypsin inhibitor, lima bean inhibitor, and chicken ovomucoid inhibitor by anhydrotrypsin was about 80% as strong as the binding of these inhibitors by trypsin. Potato inhibitor I and pancreatic trypsin inhibitor (polyvalent) were bound equally strongly by anhydrochymotrypsin and chymotrypsin. Lima bean inhibitor was bound more strongly by anhydrochymotrypsin than by chymotrypsin. It was concluded from these results that the extremely tight binding (K_{dissn} commonly 10^{-9}–10^{-10} M) of proteinase inhibitors by proteinases (E + I $\rightleftarrows$ EI), is due primarily to a sum of weak forces in a complementary, hand-in-glove fit between proteinase and proteinase inhibitor.

Proteolytic enzyme inhibitor proteins are found in bacteria (Mahadik *et al.*, 1972), in yeast (Cabib and Farkas, 1971), in ascarides (Peanasky and Abu-Erreish, 1971), and in tissues and fluids of many higher plants and animals (Vogel *et al.*, 1968). They are apparently present for the purpose of regulating the activities of endogenous proteinases or for the purpose of protecting the organisms against digestion by foreign proteinases.

In 1965 Laskowski hypothesized that the trypsin–soybean trypsin inhibitor complex involved an acyl-enzyme (Finkenstadt and Laskowski, 1965). Subsequently, a great deal of evidence was obtained for an acyl bond in a great number of enzyme–inhibitor complexes (Laskowski and Sealock, 1971). This striking feature of proteinase–proteinase inhibitor complexes suggested a functional role for the acyl linkage, *i.e.*, a stabilizing role. This suggestion, involving obligatory acyl-enzyme–inhibitor formation, has been questioned for a long

† From the Department of Agricultural Chemistry and the Department of Chemistry, Washington State University, Pullman, Washington 99163. *Received April 11, 1973.* Supported in part by U. S. Public Health Service Grants 2K3 GM 17059 and GM 12505, and U. S. Department of Agriculture C.S.R.S. Grant 916-15-29, and U. S. Public Health Service Grant AM 02299. Scientific Paper No. 4048, Project 1791, College of Agriculture Research Center, Washington State University, Pullman, Wash. 99163.

‡ Present address: Department of Biochemistry, University of Washington, Seattle, Wash. 98195.
§ U. S. Public Health Service Career Development awardee.